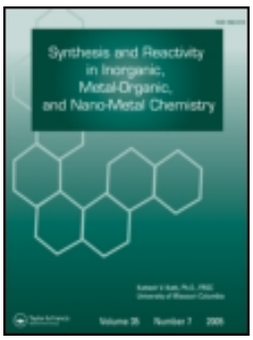

Synthesis and Reactivity in Inorganic, Metal-Organic, and Nano-Metal Chemistry

ISSN: 1553-3174 (Print) 1553-3182 (Online) Journal homepage: https://www.tandfonline.com/loi/lsrt20

Fabrication, Characterization, and Growth Mechanism of Cobalt Oxide Nanodots to Nanospheres *Via* Soft Chemical Solution Process

Manawwer Alam, Naushad Ahmad & Rizwan Wahab

To cite this article: Manawwer Alam, Naushad Ahmad & Rizwan Wahab (2016) Fabrication, Characterization, and Growth Mechanism of Cobalt Oxide Nanodots to Nanospheres *Via* Soft Chemical Solution Process, Synthesis and Reactivity in Inorganic, Metal-Organic, and Nano-Metal Chemistry, 46:9, 1318-1323, DOI: 10.1080/15533174.2015.1068807

To link to this article: https://doi.org/10.1080/15533174.2015.1068807

Accepted author version posted online: 25 Jan 2016.
Published online: 14 Apr 2016.

Synthesis and Reactivity in Inorganic, Metal-Organic, and Nano-Metal Chemistry (2016) 46, 1318–1323

ISSN: 1553-3174 print / 1553-3182 online
DOI: 10.1080/15533174.2015.1068807

Taylor & Francis
Taylor & Francis Group

Fabrication, Characterization, and Growth Mechanism of Cobalt Oxide Nanodots to Nanospheres *Via* Soft Chemical Solution Process

MANAWWER ALAM[1], NAUSHAD AHMAD[2], and RIZWAN WAHAB[3]

[1]*Research Centre, College of Science, King Saud University, Kingdom of Saudi Arabia*
[2]*Department of Chemistry, College of Science, King Saud University, Riyadh, Kingdom of Saudi Arabia*
[3]*Department of Zoology, College of Science, King Saud University, Riyadh, Kingdom of Saudi Arabia*

Received 15 March 2014; accepted 31 May 2015

In this study, the authors report a facile synthesis for the formation of nanoscale CoO dots to nanospheres via solution technique at low temperature and characterized in terms of their morphological, structural, compositional, and thermal properties. The morphological characterizations of as-synthesized and annealed CoO structures were done by scanning electron microscopy (SEM) and transmission electron microscopy, which confirmed that synthesized products are very small in size and bears small dots to spheres such as structures. The surface of nanodots is smooth and clean throughout the whole morphology. The crystalline property was analyzed with X-ray diffraction pattern and it reveals that the formed structures exhibit small size and clearly consistent with SEM observation. The compositional and thermal properties of as-synthesized and annealed CoO structures were observed *via* Fourier transform infrared spectroscopy and Thermogravimetric analysis, which confirmed that synthesized structures are pure CoO and showed good thermal stability. Finally, plausible mechanisms for the formation of CoO nanodots to nanospheres are also discussed.

Keywords: nanodots, nanospheres, cobalt oxide, thermogravimetric analysis, X-ray diffraction pattern

Introduction

It is worldwide recognized that superior properties of nanomaterials provided promise a revolutionary and new approach with a major impact in various innovative applications. Metal oxides, in particular, provide a fundamental stepping stone for the development of functional nanomaterials. In an oxidative environment, oxides are the lowest free energy states for most metals in the periodic table and demonstrate applications ranging from semiconductors to insulators.[1] In response to the increasing demands for clean energy technologies, super capacitors are considered to be the most promising energy storage and power output technologies for portable electronics, electric vehicles, and renewable energy systems operated on intermittent sources such as the sun and the wind.[2] Among the various candidates as electrode materials of super capacitor, transition metal oxides are paid special attention. For example, RuO_2 and IrO_2 exhibited prominent properties as pseudo capacitive electrode materials.[3,4] However, high cost of these materials usually limited them from wide applications. Therefore, scientists have been developing various cheap alternatives (e.g., NiO_x, CoO_x, MnO_2.[5–7] Compared with RuO_2, these oxides exhibited lower electrochemical capacitance performance due to the poor conductivity. Therefore, exploring effective techniques to improve the capacitor performance of these materials is becoming one of the most active research themes. Mutual interactions and combination of transition metal oxides give rise to their superior electrical, magnetic, and catalytic properties due to complex structure formation.[8] Copper–cobalt oxide thin films have found applications in solid-state optical gas sensors,[9] solar collectors,[10] and catalysts in electrochemical devices.[11] However, the unique catalytic, magnetic, photonic, and electrochemical properties of these nanostructured metal oxides are environmentally sustainable. The screening and synthesis of new nanostructured metal oxides is a major research topic among various research groups and extremely challenging, as they do not often conform to the principles of green chemistry. The utilization of different surfactants such as oleic acid, trioctylphosphineoxide, octadecylamine, and trioctylphosphine has been reported lead differences in reaction pathways and reaction intermediates, prior to the nucleation, leading to the formation of nanoparticles/dots with very different properties.[12] Replacement of such synthesis methodologies with environment friendly

Address correspondence to Manawwer Alam Research Centre, College of Science, P. O. Box-2455, King Saud University, Kingdom of Saudi Arabia Email: malamiitd@gmail.com
Color versions of one or more of the figures in the article can be found online at www.tandfonline.com/lsrt.

sustainable process provides advantages of easy integration into biological processes.[13] Materials based on cobalt oxides has attracted tremendous attention due to its distinct structure, properties and potential technological application in many fields such as solid or gas state sensors, magnetic fluids, catalysts, information storage, imaging, anodes of lithium-ion batteries and electrochemical properties.[14–19] The properties requires for these applications are oxidation state and size dependent. Cobaltous oxide (CoO), an absolutely necessary additive in anode of Ni/H_2 and Ni/Cd batteries, is a low-valence transition metal oxide. The low crystal anisotropy of cobalt also promotes their study them as a model system for the effects of size, shape, crystal structure, and surface anisotropy on their macroscopic magnetic response. CoO nanocrystals also have been explored as a component of multioxide catalyst or a single catalyst for hydrodesulfurization[20] and CO oxidation,[21] synthesized CoO nanocubes, and electrochemical behaviors.[14] Wang et al.[16] reported the synthesis of octahedral CoO nanocrystals with sizes of 200 nm or even larger and characterized the electrochemical performance. Zhang et al.[22] prepared CoO nanocrystals with various morphologies by turning surfactant concentration. It is important to mention that pure CoO is difficult to obtain by a simple chemical route since this approach typically produces CoO with small amount of $Co_3O_4$and Co metal. CoO nanoparticles were prepared from high-purity cobalt metal by a laser vaporization controlled condensation.[23]

In this article, we report a new simple and mild procedure to synthesize pure CoO nanodots to nanospheres involving reaction between cobalt acetate tetrahydrate $(Ac)_2Co.4H_2O)$ and sodium hydroxide (NaOH) in solvent methanol under soft solution process. The size and shape of synthesized structures were controlled by reaction temperature. This study focuses on the modulation of synthetic parameters and arrangement of cobalt nanodots to nanospheres.

Experimental

Synthesis of Cobalt Oxide (CoO-NDs) Nanodots to Nanospheres (CoO-NSs)

All reagents were purchased from Sigma–Aldrich and used without further purification. The synthesis of CoO-NDs were performed with using cobalt acetate tetrahydrate, sodium hydroxide (NaOH) and deionized water. Cobalt acetate tetrahydrate and sodium hydroxide were mixed in 50 mL of deionized water to a final concentration of 10 mM (0.12454 g) and 0.2 M (0.20 g), respectively under constant stirring for 30 min. The pH of the solution was measured and controlled using ion analyzer (corning pH meter 430 red, Cole-Parmer, USA) till it reached up to 12.30. After the complete dissolution, solution was transferred in to a refluxing pot and refluxed at 90°Cfor 1 h. As the refluxing temperature increases, the color of the solution changes from dark red to black. After refluxing, the precipitate was washed to remove the ionic impurities with methanol, ethanol and acetone several times, dried at room temperature. The dried as-grown sample was again annealed (Nabertherm, Inc. New Castle, DE) at 300°C for 1 h for at a ramp rate of 5°C/min, and was characterized in terms of their structural and chemical properties. The sample was annealed to remove the ionic impurities and get pure materials.

Characterization

The morphological observations of black colored as-grown and annealed powder were made by a scanning electron microscopy (SEM; JSM-6380 LA, Japan). For SEM observation, the powder was uniformly spread on a carbon tape and coated with thin conducting layer of platinum for 3 s. The crystallinity and phases of the black colored powder was characterized with X-ray powder diffractometer (XRD; PANalytical XPert Pro, USA) with $Cu_{K\alpha}$ radiation ($\lambda = 1.54178$ Å) in the range of 20–60° with 6°/min scanning speed. The morphological properties of as-grown and annealed samples were examined with the use of SEM at room temperature (Jeol, JED-2200 series, Japan). For more clarification related to morphology and crystalline character, the grown nanostructure of cobalt was analyzed with transmission electron microscopic measurement (TEM). For TEM (JEOL JEM-2100F, Japan) measurement, nanostructures of black cobalt powder was sonicated in an alcohol (ethanol) solvent for 10–15 min and then a carbon-coated copper grid (400 mesh) was dipped in a suspension solution of cobalt nanostructures and dried at room temperature and structural morphology was analyzed at 200 kV. The thermal analysis (TGA) was performed using TGA/DSC1 instrument (Mettler Toledo AG, Analytical CH-8603,Schwerzenbach, Switzerland). For thermal analysis, about 5 mg of the sample was loaded into alumina crucibles (Al_2O_3) in the heating zone of the TGA. The thermal scanning mode ranges from ambient temperature to 800°C at a programming heating rate of 20°C/min under nitrogen gas with flow 20 mL/min. The chemical compositions of as-synthesized and annealed powder were examined by using Fourier transform infrared (FTIR; PerkinElmer-FTIR Spectrum-100) in the range of 400–4000 cm^{-1}.

Results and Discussion

Morphological Investigation of CoO-NDs and CoO-NSs Via SEM

To investigate the general morphologies of as-synthesized and annealed nanopowder were characterized by SEM and results are shown in Figures 1a and 1b. It is apparent from the low magnified image as-synthesized particles are in very small size with an agglomerated form. The diameter of nanodots (CoO-NDs) is in the range of 20 ± 5 nm, whereas each array of nanoclusters is in the range of 2–3 μm. As the powder was annealed at 300°C for 1 h and cooled at room temperature. The synthetic impurities

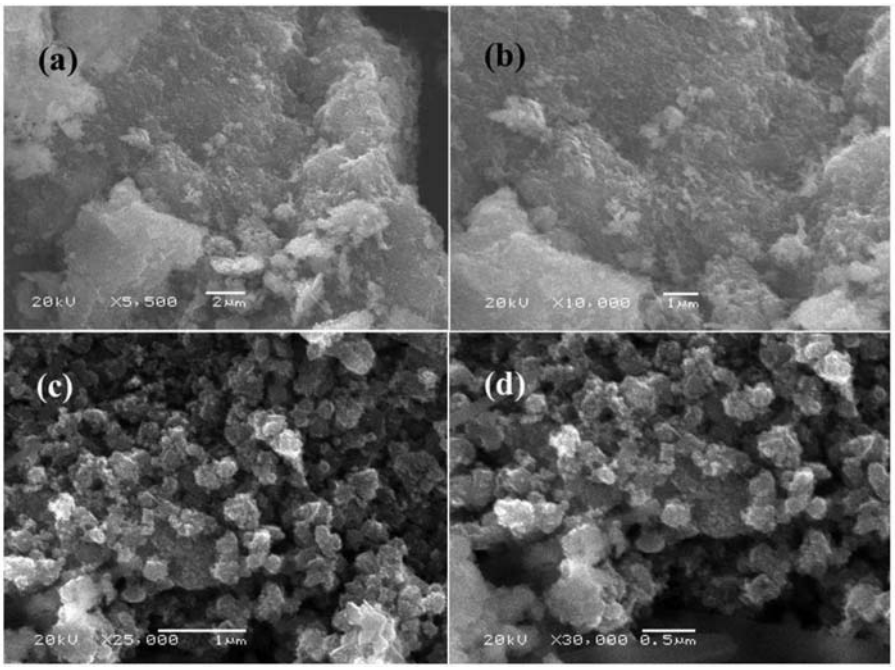

Fig. 1. Typical low and high (a,b) magnified SEM images of as-grown cobalt oxide nanodots and spheres (c,d) of cobalt oxide annealed at 300°C for 1 h.

were removed completely and pure CoO-NSs have been obtained. Figures 1c and 1d exhibit typical low- and high-magnified images that confirm that CoO-NSs are synthesized in high density and possess small size nanosphere (NS) structures. The spheres were made by the accumulation of several small nanodots particles. Interestingly, it is seen that the surface of each nanodots are jointed with other in such a manner that they make multishaped sphere structures. The typical diameters of nanorods are in the range of 45 ± 5 nm, while each array sphere is in the range of 2–3 μm (Figure 1d).

TEM

The structures morphology of grown nanostructures of cobalt was further identified via TEM equipped with high-resolution TEM (HR-TEM). Figures 2a and 2b show the low magnifi-

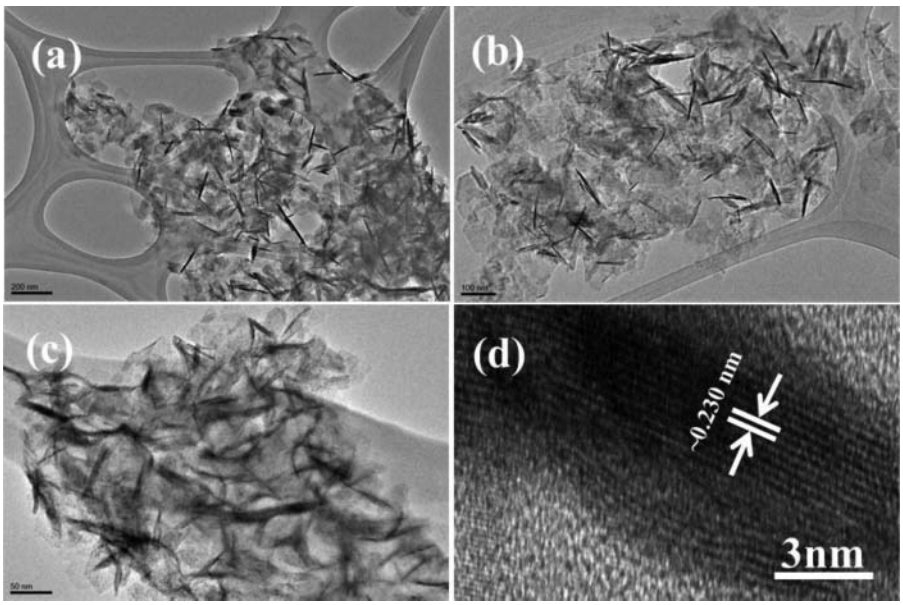

Fig. 2. (a,b) Low- and (c) high-magnification TEM image of cobalt oxide nanostructures and (d) their corresponding HR-TEM image, which presents the lattice variance between two fringes are about ~0.230 nm.

cation transmission electron microscopic images, where as Figure 2c shows high magnified image of cobalt oxide nanopowder. Several nano shaped particles (NPs) are seen at low magnification (Figures 2a and 2b). The size of each nano shaped particle is in the range of 25–30 nm. The high magnification (Figure 2c) image shows the particles having smooth, aggregated surfaces, which is clearly consisted with observed data of SEM images. The crystalline character of grown nanostructures was observed with HR-TEM (Figure 2d) shows the lattice fringe between two adjacent planes is about 0.230 nm, which is closely related to previously published literature.[24–26] The size, shapes and crystalline property of grown nanoparticles observed from TEM analysis (Figures 2a and 2b) and are in consistent with X-ray diffraction (Figure 3) pattern and SEM images (Figure 3).[24–26]

XRD

Figure 3 shows typical XRD patterns of grown and annealed nanodots obtained at the previous synthetic conditions. Well-defined dominant diffraction reflection peaks are seen in the observed XRD spectra, which are related to the face centered cubic structures (JCPDS card No. 071-1178) and are well matched with cobalt oxide. The as-grown sample peaks at 2θ angle of 37.53 and 43.77 can be assigned the major lattice scattering plane 111 and 200 for CoO crystal (Figure 3a), the data are in agreement with previously published literature of pure cobalt oxide.[27,28] The crystal size was found to be 20 ± 5 nm, which matches the results obtained from SEM. The sharp diffraction peaks indicates that as-synthesized CoO particles exhibit good crystallinity, while the qualitatively broader peak widths indicate that particles have a smaller size. As compared to the as-grown CoO particles, in the annealed (Figure 3b), the peaks become sharper and intensity rises, respectively. As we know that sharper peaks in XRD patterns mean bigger crystal grains. Only one peak in XRD defines that obtained crystals are single crystalline and highly pure oxide crystals (Figure 3b). Thus, there is no evidence for existence of crystalline impurities based on XRD.

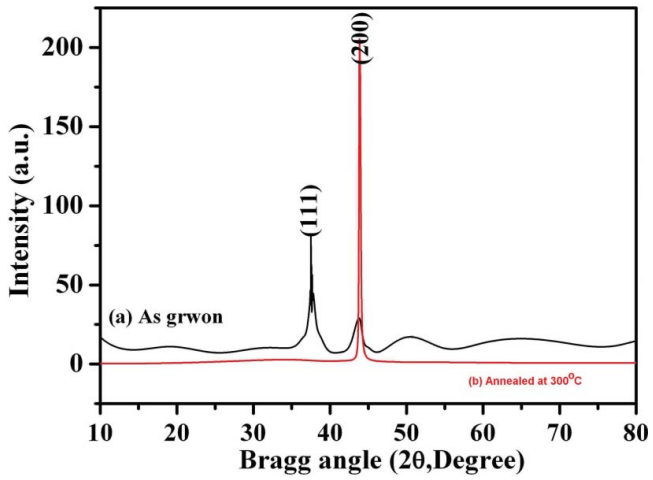

Fig. 3. X-ray diffraction pattern (XRD) of synthesized cobalt oxide nanodots: (a) as-grown(b) annealed powder of cobalt oxide nanospheres prepared at 300°C.

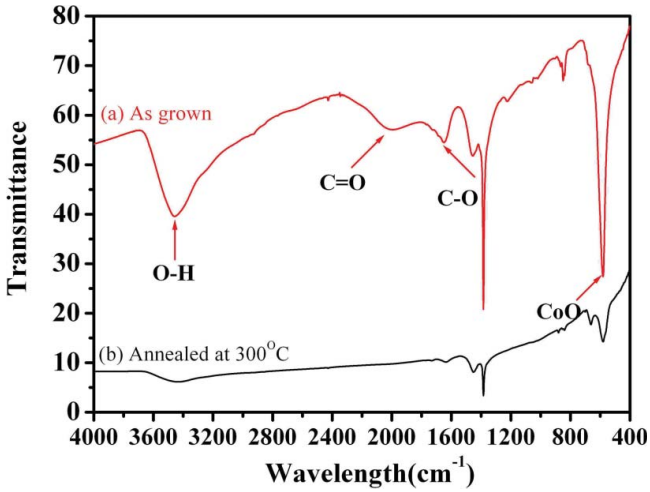

Fig. 4. FTIR spectra of synthesized cobalt oxide (a) as-grown (Co-NDs) and (b) annealed (Co-NSs) at 300°C.

Compositional Analysis by FTIR Spectroscopy

To determine the chemical composition of as-synthesized CoO-NDs and CoO-NSs. plots in Figure 4a and 4b are the FTIR absorption spectra of as-grown and annealed CoO structures, respectively. In as-grown structures (Figure 4a), the strong absorption at about 1742 cm^{-1} is attributed to the typical absorption of C = O stretch vibration of saturated acetate ions. The peak at 1047 cm^{-1} can be indexed to C–O–C symmetric stretch vibration, while slight broad strong peak at 1255 cm^{-1} is of C–O–C asymmetric stretch vibration. The presence of small absorption band at 1623 cm^{-1} can be related with bending vibration of absorbed water and surface hydroxyl[28] while peak appeared at 3525 cm^{-1} is related to the O-H stretching mode.[29,30] No other absorption band related with any other functional group was detected in the FTIR spectrum which reveals that annealed CoO nanospheres possess good purity without any significant impurity (Figure 4b). The absorption band observed near 530 cm^{-1} is may be due to the presence of metal–oxygen bond which confirm the formation of CoO-NSs.[31] The presence of small peak at 885 cm^{-1} was generally observed in the FTIR spectrum, if the samples are measured in air.[32]

TGA

The thermal decomposition of as-synthesized (CoO-NDs) and annealed (CoO-NSs) have been examined by TGA, performed under nitrogen flow(20 mL/min), at a heating rate of 20°C/min. The TGA curve shows three stages of weight loss in terms of temperature (Figure 5a). The first step starts at 125°C and is completed at 165°C with a weight loss of 14.94%. The second and major one begins at 165°C and is completed at 345°C with 23.87% weight loss followed by final and small weight loss at 454°C, resulting in a residue amounting to 28.90% of the initial weight loss (Figure 5b). The annealed nanostructures were stable and very less mass loss was observed as compared to as-grown nanostructures. As

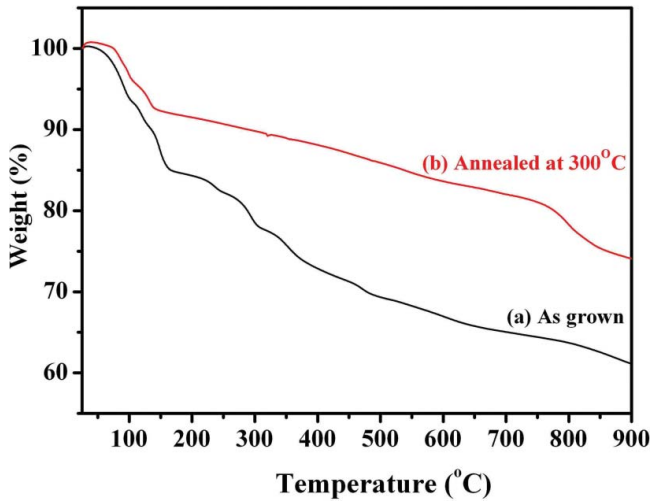

Fig. 5. Thermogravimetric analysis of the decomposition of (a) as-synthesized and (b) annealed cobalt oxide with over the temperature range 25–800°C.

can be seen in thermogram (Figure 4b) that at 345°C weight loss was 10.94%, whereas it increases to 13.04% at 454°C. The obtained clearly justified that grown and annealed nanostructures are stable at higher temperature. These results are in good agreement with XRD and FTIR studies from both the as-grown and annealed samples.

Possible Proposed Mechanism for the Formation of Cobalt Oxide Nanodots to Nanospheres

The soft chemical reaction synthesis is a technique by which we can prepare various types of materials such as metal oxide, composite, organic-inorganic etc, at a relatively low temperature, consists of hydrolysis of the constituent molecular precursor and subsequent poly condensation for the synthesis of various types of metal oxides. When an aqueous solution of salt cobalt ($Co(Ac)_2.4H_2O$) reacts with alkali (NaOH) under an aqueous medium and precipitate out of the solution. On the basis of their synthesis and characterization of the prepared materials such as XRD pattern, FTIR, SEM, and thermal analysis a simple chemical reaction mechanism has been developed. We have discussed here, the formation mechanism of cobalt oxide nanodots (Co-NDs) to nanospheres (Co-NSs) grown at a very low refluxing temperature (90°C) and annealed at 300°C for 1 h, respectively. Initially, when the solution of cobalt acetate tetrahydrate was dissolved under constant stirring a dark red colored was formed and alkali (0.2M NaOH) was poured drop by drop, the color of solution was changed to ultimately wine red colored. At this time the pH of solution was measured, which reached 12.3. The wine red solution of cobalt acetate tetrahydrate ($(Ac)_2Co.4H_2O$) and sodium hydroxide (NaOH) was transferred to two-necked refluxing pot and refluxed at 90°C for 1h on hot plate. As the reaction proceeds with increase of temperature, wine colored solution changes to black colored within 15–20 min. During the precipitation/solution process, sodium hydroxide played an important role in nucleation and growth of nanodots. In solution hydroxyl (OH^-) ions from sodium hydroxide reacts with acetate chain of cobalt and form cobalt hydroxide($Co(OH)_2$) and sodium acetate (CH_3COONa)as Eq. 1. As the temperature of refluxing pot increases and reached to their optimum level hydroxide molecule of cobalt changes to oxide form and makes cobalt oxide (CoO) as Eq. 2. The small dots are formed in black solution (Figure 5a). The bigger dots are cobalt oxide dots where as smaller dots are hydroxide molecule of CoO (Figure 6a). In solution, as the refluxing temperature rises, hydroxide molecule changes to oxide molecules. The nanodots was purified with solvents such as methanol, ethanol and acetone dried at room temperature and further annealed to improve crystallinity and quality of material at 300°C for 1 h (Figures 6b and 6c). At high temperature the small dots were colloids with each other and form a giant molecule of nanodots

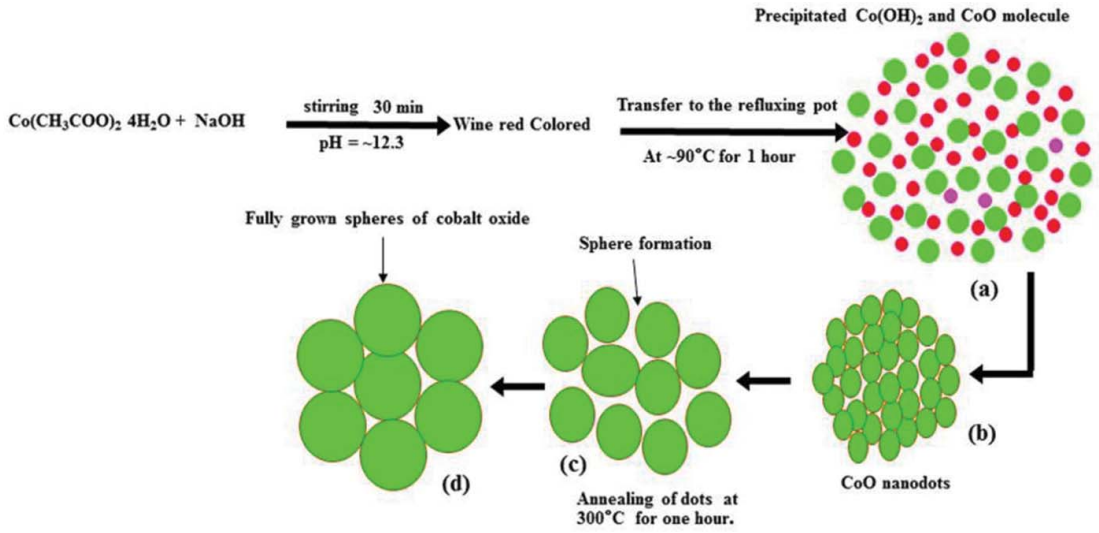

Fig. 6. Possible proposed mechanism for the formation of CoO-NDs to Co-NSs.

(Figure 6d). This giant morphology having sphere like morphology and forms spheres of cobalt oxide (Figure 6d). In this experiment, we have observed that refluxing and annealing time are very important parameters for the formation and stability of the nanostructures because at optimum refluxing time, nanostructures are stable but when the refluxing or annealing time is exceeded, the molecules gets merged with each other and form diverse shaped nanostructures.

$$Co(CH_3COO)_2 \cdot 4H_2O + 2NaOH \rightarrow Co(OH)_2 + 2CH_3COONa + 4H_2O \quad (1)$$

$$Co(OH)_2 \rightarrow CoO + H_2O \quad (2)$$

Conclusions

We have controlled a reaction parameter to fabricate pure CoO-NDs to CoO-NSs with nearly uniform shape and particle size by reaction between cobalt acetate and sodium hydroxide in an aqueous media. The synthesized nanostructures were characterized with standard characterization techniques such as XRD pattern, SEM, and TEM equipped with HR-TEM for morphology. The composition and thermal stability of prepared materials were analyzed within detail in terms of their morphological, structural, compositional, and optical properties.

Funding

This project was supported by King Saud University, Deanship of Scientific Research, College of Science-Research Center.

References

1. Henrich, V. E.; Cox, P. A. *The Surface Science of Metal Oxides*; Cambridge University Press: Boston, MA, **1994**.
2. Wang, D. W.; Li, F.; Chen, Z.-G.; Lu, G. Q.; Cheng, H. M. *Chem. Mater.* **2008**, *20*, 7195–7200.
3. Zheng, J. P.; Cygan, P. J.; Jow, T. R. J. *Electrochem. Soc.* **1995**, *142*, 2699–2703.
4. Krysa, J.; Mraz, R. *Electrochim. Acta* **1995**, *40*, 1997–2003.
5. Wang, Y. G.; Zhang, X. G. *J. Electrochem. Soc.* **2005**, *152*, A671–A676.
6. Jeong, X. U.; Manthiram, A. *J. Electrochem. Soc.* **2002**, *149*, 1419–1422.
7. Rong, X.; Zheng, H. C. *Langmuir* **2004**, *20*, 9780–9790.
8. Wojciechowska, M.; Zielinski, M.; Malczewska, A.; Przystajko, W.; Pietrowski, M. *Appl. Catal. A: Gen.* **2006**, *298*, 225–231.
9. Ando, M.; Kobayashi, T.; Iijima, S.; Haruta, M. *J. Mater. Chem.* **1997**, *7*, 1779–1781.
10. Skumryev, V.; Stoyanov, S.; Zhang, Y.; Hadjipanayis, G.; Givord Nogues, D. J. *Nature* **2003**, *423*, 850–853.
11. Nakaoka, K.; Nakayama, M.; Ogura, K. *J. Electrochem. Soc.* **2002**, *149*, C159–C163.
12. De Silva, R. M.; Palshin, V.; de Silva, K. M. N.; Henry, L. L.; Kumar, C. S. S. R. *J. Mater. Chem.* **2008**, *18*, 738–747.
13. Blanco-Andujar, C.; Tung, L. D.; Thanh, N. T. K. *Ann. Rep. Prog. Chem., Sect. A: (Inorg. Chem)*. **2010**, *106*, 553–568.
14. Nam, K. M.; Shim, J. H.; Han, D. W.; Kwon, H. S.; Kang, Y. M.; Li, Y.; Song, H.; Seo, W. S.; Park, J. T. *Chem. Mater.* **2010**, *22*, 4446–4454.
15. Choudhary, V. R.; Jhaa, R.; Janaa, P. *Catal. Commun.* **2008**, *10*, 205–207.
16. Wang, D.; Ma, X.; Wang, Y.; Wang, L.; Wang, Z.; Zheng, W.; He; X.; Li, J.; Peng, Q.; Li, Y. *Nano Res.* **2010**, *3*, 1–7.
17. Wang, G. X.; Chen, Y.; Konstatinov, K.; Lindsay, M.; Liu, H. K.; Dou, S. X. *J. Power Sources* **2002**, *109*, 142–147.
18. Choi, H. C.; Lee, S. Y.; Kim, S. B.; Kim, M. G.; Lee, M. K.; Shin, H. J.; Lee, J. S. *J. Phys. Chem. B* **2002**, *106*, 9252–9260.
19. Do, J. S.; Weng, C. H. *J. Power Sources* **2005**, *146*, 482–486.
20. Bartsch, R.; Tanielian, C. *J. Catal.* **1974**, *35*, 353–358.
21. Teng, Y.; Sakurai, H.; Ueda, A.; Kobayashi, T. *Int. J. Hydrogen Energy* **1999**, *24*, 355–358.
22. Zhang, Y.; Zhu, J.; Song, X.; Zhong, X. *J. Phys. Chem. C* **2008**, *112*, 5322–5327.
23. Glaspell, G. P.; Jagodzinski, P. W.; Manivannan, A. *J. Phys. Chem. B* **2004**, *108*, 9604–9607.
24. Knappett, B. R.; Abdulkin, P.; Ringe, E.; Jefferson, D. A.; Lozano-Perez, S.; Rojas, T. C.; Fernández, A.; Wheatley, A. E. H. *Nanoscale* **2013**, *5*, 5765–5772.
25. He, M.; Jiang, H.; Liu, B.; Fedotov, P. V.; Chernov, A. I.; Obraztsova, E. D.; Cavalca, F.; Wagner, J. B.; Hansen, T. W.; Anoshkin, I. V.; Obraztsova, E. A.; Belkin, A. V.; Sairanen, E.; Nasibulin, A. G.; Lehtonen, J.; Kauppinen, E. I. *Sci. Reports* **2013**, *3*, Artcle no. 1460.
26. Salazar-Alvarez, G.; Sort, J.; Uheid, A.; Muhammed, M.; Suriñach, S.; Baróa, M. D.; Nogués, J. *J. Mater. Chem.* **2007**, *17*, 322–328.
27. Gupta, R. K.; Sinha, A. K.; Sekhar, B. N. R.; Srivastava, A. K.; Singh, G.; Deb, S. K. *Appl. Phys. A: Mater. Sci. Process.* **2011**, *103*, 13–19.
28. Nidhin, N.; Sreeram, K. J.; Nair, B. U. *Chem. Eng.* **2012**, *185*, 352–357.
29. Al-Hajry, A.; Umar, A.; Hahn, Y. B.; Kim, D. H. *Superlatt. Microstruct.* **2009**, *45*, 529–534.
30. Nyquist, R. A.; Kagel, R. O. *Infrared Spectra of Inorganic Compounds*; Academic Press, Inc.: New York, 1971.
31. Polarz, S.; Orlov, A.; van den Berg, V. M. W. E.; Driess, M. *Angew. Chem., Int. Ed.* **2005**, *44*, 7892–7896.
32. Umar, A.; Rahman, M. M.; Al-Hajry, A.; Hahn, Y. B. *Talanta* **2009**, *78*, 284–289.